

Notes on Advection

These notes introduce the basic numerical methods for dealing with advection, using finite-volume techniques.

1 First-order advection in one-dimension via finite-differences

The linear advection equation is simply:

$$a_t + ua_x = 0 \quad (1)$$

where $a(x, t)$ is some scalar quantity and u is the velocity at which it is advected ($u > 0$ advects to the right). The solution to Eq. 1 is to simply take the initial data, $a(x, t = 0)$, and displace it to the right at a speed u . The shape of the initial data is preserved in the advection. Many hyperbolic systems of PDEs, e.g. the equations of hydrodynamics, can be written in a form that looks like a system of (nonlinear) advection equations, so the advection equation provides important insight into the methods used for these systems.

Exercise 1: Show that $a(x - ut)$ is a solution to Eq. 1 for any choice of a . This means that the solution is constant along the lines $x = ut$.

To get a flavor of the methods for advection, we will use a simple finite-difference discretization—here, the domain is divided into a sequence of points where we store the solution. We will solve Eq. 1 numerically by discretizing the solution at these points. The index i denotes the point's location, and a_i denotes the discrete value of $a(x)$ in zone i . The data in each zone can be initialized as $a_i = a(x_i)$. Figure 1 shows the grid.

We also need to discretize in time. We denote the time-level of the solution with a superscript, so $a_i^n = a(x_i, t^n)$. For a fixed Δt , time level n corresponds to a time of $t = n\Delta t$.

A simple first-order accurate discretization is:

$$\frac{a_i^{n+1} - a_i^n}{\Delta t} = -u \frac{a_i^n - a_{i-1}^n}{\Delta x} \quad (2)$$

This is an *explicit* method, since the new solution, a_i^{n+1} , depends only on information at the old time level, n .

Finally, we also need to specify a boundary condition for this. Our choice of spatial derivative is one-sided—it uses information from the zone to the left of the zone we are updating. This is because information is flowing from left to right in this problem ($u > 0$). This choice of the derivative is called *upwinding*—this choice of derivative results in a stable method. Notice that if we use Eq. 2 to update the data in the first zone inside the boundary, we need data to the left of this zone—outside of the domain. This means that we need a single ghost point to implement the boundary conditions for our method. The presence of the ghost points allow us to use the same update equation (e.g. Eq. 2) for all zones in the domain.

The last piece of information needed to update the solution is the timestep, Δt . It can be shown that for the solution to be *stable*, the timestep must be less than the time it takes information to propagate across a single zone. That is:

$$\Delta t \leq \frac{\Delta x}{u} \quad (3)$$

This is called the *Courant-Friedrichs-Lewy* or *CFL* condition. A dimensionless quantity called the *CFL number* is defined as

$$C = \frac{\Delta t u}{\Delta x} \quad (4)$$

Stability requires $C \leq 1$. We traditionally write the timestep as

$$\Delta t = C \frac{\Delta x}{u} \quad (5)$$

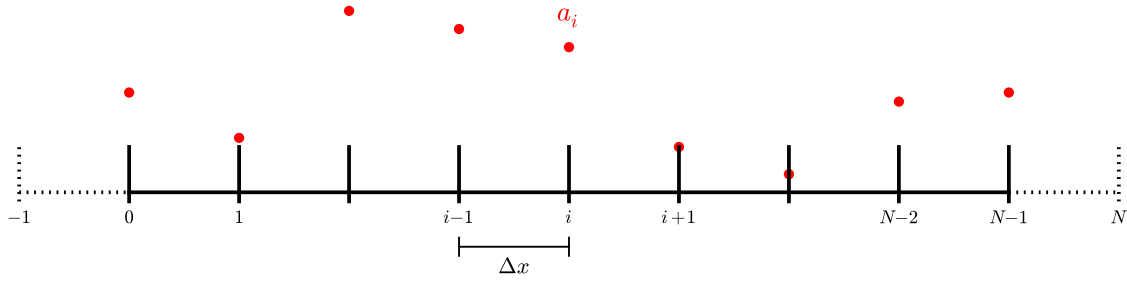


Figure 1: A simple finite-difference grid. The solution is stored at each of the labeled points. The dotted lines show the ghost points used to extend our grid past the physical boundaries to accommodate boundary conditions. Note that if we are periodic, then points 0 and $N - 1$ are at the same physical point in space, so we would only need to update one of them.

and specify C as part of the problem (a typical value may be $C = 0.7$).

Exercise 2: Show analytically that when you use $C = 1$ in the first-order differenced advection equation (Eq. 2) that you advect the profile exactly, without any numerical error.

Keep in mind that, in general, we will be solving a non-linear system of equations, so it is not possible to run with $C = 1$, since u (and therefore C) will change from zone to zone. Instead, one looks at the most restrictive timestep over all the zones and uses that for the entire system.

Exercise 3: Write a code to solve the 1-d linear advection equation using the discretization of Eq. 2 on the domain $[0, 1]$ with $u = 1$ and periodic boundary conditions. For initial conditions, try both a Gaussian profile and a top-hat:

$$a = \begin{cases} 0 & \text{if } x < 1/3 \\ 1 & \text{if } 1/3 \leq x < 2/3 \\ 0 & \text{if } 2/3 \leq x \end{cases} \quad (6)$$

Note: For a general treatment of boundary conditions, you would initialize the ghost points to their corresponding periodic data and apply the difference equations to zones $0, \dots, N - 1$. However, for periodic BCs on this grid, points 0 and $N - 1$ are identical, so you could do the update in this special case on points $1, \dots, N - 1$ without the need for ghost points and then set $a_0 = a_{N-1}$ after the update.

Run your program for one or more periods (one period is $T = 1/u$) with several different CFL numbers and notice that there is substantial numerical dissipation.

Exercise 4: You may think that using a centered-difference for the spatial derivative, $u_x \sim (u_{i+1} - u_{i-1})/(2\Delta x)$ would be more accurate. This method is called FTCS (forward-time, centered-space). Try this. You will find that the solution is unconditionally unstable.

The classic method for understanding stability is to consider the growth of a single Fourier mode in our discretization. That is, substitute in $a_i^n = A^n e^{ji\theta}$, where $j = \sqrt{-1}$, and θ represents a phase. A method is stable if $|A^{n+1}/A^n| \leq 1$. Performing this with FTCS shows that no value of C can make the method stable. Doing the same analysis for Eq. 2 would show that the upwind method is stable for $0 \leq C \leq 1$. (Note that this stability analysis only works for linear equations, where the difference Fourier modes are decoupled, nevertheless, we use its ideas for nonlinear advection problems as well).

Exercise 5: To get an alternate feel for stability, we can ask what the terms left out by truncation look like. That is, we can begin with the discretized equation:

$$a_i^{n+1} - a_i^n = -\frac{u\Delta t}{\Delta x}(a_i^n - a_{i-1}^n) \quad (7)$$

and replace a_i^{n+1} with a Taylor expansion in time, and replace a_{i-1}^n with a Taylor expansion in space, keeping terms to $O(\Delta t^3)$ and $O(\Delta x^3)$. Replacing $\partial a / \partial t$ with $-u\partial a / \partial x$ in the higher-order terms, show that our difference equation more closely corresponds to

$$a_t + ua_x = \frac{u\Delta x}{2} \left(1 - \frac{\Delta t u}{\Delta x}\right) \frac{\partial^2 a}{\partial x^2} \quad (8)$$

$$= \frac{u\Delta x}{2}(1 - C) \frac{\partial^2 a}{\partial x^2} \quad (9)$$

Notice that the righthand side looks like a diffusion term, however, if $C > 1$, then the coefficient of the diffusion is negative—this is unphysical. This means that the diffusion would act to take smooth features and make them more strongly peaked—the opposite of physical diffusion.

An alternate approach to time-discretization is to do an implicit discretization. Here our upwind method would appear as:

$$\frac{a_i^{n+1} - a_i^n}{\Delta t} = -u \frac{a_i^{n+1} - a_{i-1}^{n+1}}{\Delta x} \quad (10)$$

We can write this as a linear system with coupled equations:

$$-Ca_{i-1}^{n+1} + (1 + C)a_i^{n+1} = a_i^n \quad (11)$$

This requires a matrix solve—this makes implicit methods generally more expensive than explicit methods. However, stability analysis would show that this implicit discretization is stable for any choice of C . (But one must not confuse stability with accuracy—the most accurate solutions with this method will still have a small C).

2 Second-order advection in one-dimension and the finite-volume method

We will typically use a *finite-volume* discretization of the advection equation. First we rewrite the advection equation in *conservation form*:

$$a_t + [f(a)]_x = 0 \quad (12)$$

where $f(a) = ua$ is the flux of the quantity a . In conservation form, the time derivative of a quantity is related to the divergence of its flux.

Recall that in the finite-volume discretization, $\langle a \rangle_i$ represents the average of $a(x, t)$ over the interval $x_{i-1/2}$ to $x_{i+1/2}$, where the half-integer indexes denote the zone edges (i.e. $x_{i-1/2} = x_i - \Delta x/2$). Figure 2 shows an example of such a grid with 2 ghost cells at each end. (For simplicity of notation, we drop the $\langle \rangle$ going forward). To discretize Eq. 12, we integrate it over a zone, from $x_{i-1/2}$ to $x_{i+1/2}$, normalizing by the zone width, Δx :

$$\frac{1}{\Delta x} \int_{x_{i-1/2}}^{x_{i+1/2}} a_t dx = -\frac{1}{\Delta x} \int_{x_{i-1/2}}^{x_{i+1/2}} \frac{\partial}{\partial x} f(a) dx \quad (13)$$

$$\frac{\partial}{\partial t} a_i = -\frac{1}{\Delta x} \{ [f(a)]_{i+1/2} - [f(a)]_{i-1/2} \} \quad (14)$$

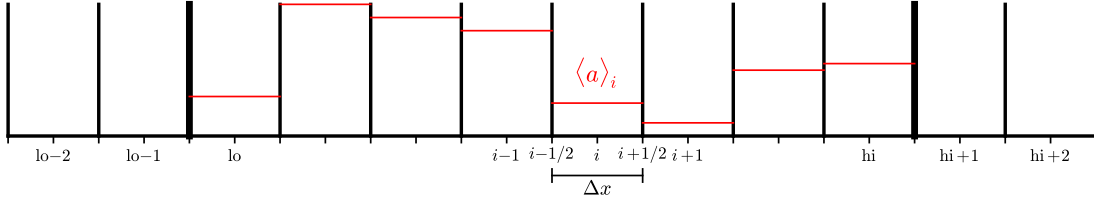


Figure 2: A finite-volume grid running from lo, \dots, hi , with two ghost cells at each end.

This is an evolution equation for the zone-average of a , and shows that it updates in time based on the fluxes through the boundary of the zone. We discretize in time by evaluating the righthand side at the midpoint in time—this gives a centered difference in time, which is second-order accurate:

$$\frac{a_i^{n+1} - a_i^n}{\Delta t} = - \frac{[f(a)]_{i+1/2}^{n+1/2} - [f(a)]_{i-1/2}^{n+1/2}}{\Delta x} \quad (15)$$

To evaluate the fluxes at the half-time, we need the state at the half-time, that is, we do :

$$[f(a)]_{i+1/2}^{n+1/2} = f(a_{i+1/2}^{n+1/2}) . \quad (16)$$

We construct a second-order accurate approximation to $a_{i+1/2}^{n+1/2}$ by Taylor expanding the data in the cell to the interface. Note that for each interface, there are two possible interface states we can construct—one using the data to the left of the interface (which we will denote with a “L” subscript) and the other using the data to the right of the interface (denoted with an “R” subscript)—see Figure 3. These states are:

$$\begin{aligned} a_{i+1/2,L}^{n+1/2} &= a_i^n + \frac{\Delta x}{2} \frac{\partial a}{\partial x} \Big|_i + \frac{\Delta t}{2} \frac{\partial a}{\partial t} \Big|_i + \mathcal{O}(\Delta x^2) + \mathcal{O}(\Delta t^2) \\ &= a_i^n + \frac{\Delta x}{2} \frac{\partial a}{\partial x} \Big|_i + \frac{\Delta t}{2} \left(-u \frac{\partial a}{\partial x} \Big|_i \right) + \dots \\ &= a_i^n + \frac{\Delta x}{2} \left(1 - \frac{\Delta t}{\Delta x} u \right) \frac{\partial a}{\partial x} \Big|_i + \dots \end{aligned} \quad (17)$$

$$\begin{aligned} a_{i+1/2,R}^{n+1/2} &= a_{i+1}^n - \frac{\Delta x}{2} \frac{\partial a}{\partial x} \Big|_{i+1} + \frac{\Delta t}{2} \frac{\partial a}{\partial t} \Big|_{i+1} + \mathcal{O}(\Delta x^2) + \mathcal{O}(\Delta t^2) \\ &= a_{i+1}^n - \frac{\Delta x}{2} \frac{\partial a}{\partial x} \Big|_{i+1} + \frac{\Delta t}{2} \left(-u \frac{\partial a}{\partial x} \Big|_{i+1} \right) + \dots \\ &= a_{i+1}^n - \frac{\Delta x}{2} \left(1 + \frac{\Delta t}{\Delta x} u \right) \frac{\partial a}{\partial x} \Big|_{i+1} + \dots \end{aligned} \quad (18)$$

A suitable estimate is needed for the slope of a that appears in these expressions (as $\partial a / \partial x$). We can approximate this simply as

$$\frac{\partial a}{\partial x} \Big|_i = \frac{a_{i+1} - a_{i-1}}{2\Delta x} \quad (19)$$

We can think of this method as reconstructing the function form of the data from the cell-average data in each cell using a piecewise linear polynomial.

We now have two states, $a_{i+1/2,L}^{n+1/2}$ and $a_{i+1/2,R}^{n+1/2}$ separated by an interface—this is called the *Riemann problem*. The solution to this will depend on the equation being solved, and results in a single state at the interface:

$$a_{i+1/2}^{n+1/2} = \mathcal{R}(a_{i+1/2,L}^{n+1/2}, a_{i+1/2,R}^{n+1/2}) \quad (20)$$

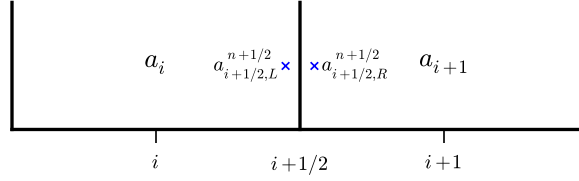


Figure 3: The left and right interface state at the $i + 1/2$ interface. Here, the left state, $a_{i+1/2,L}^{n+1/2}$, was predicted to the interface from the zone to the left of the interface, using a_i , and the right state, $a_{i+1/2,R}^{n+1/2}$, was predicted to the interface from the zone to the right, using a_{i+1} .

In our case, the advection equation simply propagates the state to the right (for $u > 0$), so the solution to the Riemann problem is to take the left state (this is another example of upwinding). That is we do:

$$\mathcal{R}(a_{i+1/2,L}^{n+1/2}, a_{i+1/2,R}^{n+1/2}) = \begin{cases} a_{i+1/2,L}^{n+1/2} & u > 0 \\ a_{i+1/2,R}^{n+1/2} & u < 0 \end{cases} \quad (21)$$

To complete the update, we use this interface state to evaluate the flux and update the advected quantity via Eq. 15.

Boundary conditions are implemented by filling the ghost cells outside each end of the domain based on data in the interior. Note that at the very left edge of the domain, the state $a_{lo-1/2}^{n+1/2}$ requires the construction of states on the left and right. The left state at that interface, $a_{lo-1/2,L}^{n+1/2}$, depends on the slope reconstructed in the $lo - 1$ ghost cell, $\partial a / \partial x|_{lo-1}$. This in turn is constructed using a limited center-difference that will consider the value in the cell to the left, $lo - 2$. Therefore, we need two ghost cells at each end of the domain for this method. Higher-order limiters may require even more ghost cells.

Exercise 6: Write a second-order solver for the linear advection equation. To mimic a real hydrodynamics code, your code should have routines for finding initializing the state, filling boundary conditions, computing the timestep, computing the interface states, solving the Riemann problem, and doing the update. The problem flow should look like:

- set initial conditions
- main evolution loop—loop until final time reached
 - fill boundary conditions
 - get timestep (Eq. 5)
 - compute interface states (Eqs. 17 and 18)
 - solve Riemann problem at all interfaces (Eq. 21)
 - do conservative update (Eq. 15)

Use both the top-hat and Gaussian initial conditions and periodic boundary conditions and compare to the first-order method.

2.1 Limiting

The second-order method likely showed some oscillations in the solution, especially for the top-hat initial conditions. *Godunov's theorem* says that any monotonic linear method for advection is first-order accurate (see, e.g, [4]). In this context, monotonic means that no new minima or maxima are introduced. The converse is true too, which suggests that in order to have a second-order accurate method for this linear equation, the algorithm itself must be nonlinear.

Exercise 7: To remove the oscillations in practice, we limit the slopes to ensure that no new minima or maxima are introduced during the advection process. There are many choices for limited slopes. A popular one is the minmod limiter. Here, we construct the slopes in the interface states as:

$$\left. \frac{\partial a}{\partial x} \right|_i = \text{minmod} \left(\frac{a_i - a_{i-1}}{\Delta x}, \frac{a_{i+1} - a_i}{\Delta x} \right) \quad (22)$$

instead of Eq. 19. with

$$\text{minmod}(a, b) = \begin{cases} a & \text{if } |a| < |b| \text{ and } a \cdot b > 0 \\ b & \text{if } |b| < |a| \text{ and } a \cdot b > 0 \\ 0 & \text{otherwise} \end{cases} \quad (23)$$

Use this slope in your second-order advection code and notice that the oscillations go away

Figure 4 shows the evolution of an initial discontinuity with and without limiting. See the text by LeVeque [5] for alternate choices of limiters. Note: most limiters will have some sort of test on the product of a left-sided and right-sided difference ($a \cdot b$ above)—this is < 0 at an extremum, which is precisely where we want to limit.

A slightly more complex limiter is the MC limiter (monotonized central difference). First we define an extrema test,

$$\xi = (a_{i+1} - a_i) \cdot (a_i - a_{i-1}) \quad (24)$$

Then the limited difference is

$$\left. \frac{\partial a}{\partial x} \right|_i = \begin{cases} \min \left[\frac{|a_{i+1} - a_{i-1}|}{2\Delta x}, 2 \frac{|a_{i+1} - a_i|}{\Delta x}, 2 \frac{|a_i - a_{i-1}|}{\Delta x} \right] \text{sign}(a_{i+1} - a_{i-1}) & \xi > 0 \\ 0 & \text{otherwise} \end{cases} \quad (25)$$

This is second-order accurate for smooth flows.

The main goal of a limiter is to reduce the slope near extrema. Figure 5 shows a finite-volume grid with the original data, cell-centered slopes, and MC limited slopes. Note that near the strong gradients is where the limiting kicks in. The different limiters are all constructed by enforcing a conditions requiring the method to be *total variation diminishing*, or TVD. More details on TVD limiters can be found in [7, 5].

A popular extension of the MC limiter is the 4th-order MC limiter, which is more accurate in smooth flows (this is shown in [2], Eqs. 2.5 and 2.6; and [3], Eq. 191).

Exercise 8: Show analytically that if you fully limit the slopes (i.e. set $\partial a / \partial x|_i = 0$, that the second-order method reduces to precisely our first-order finite-difference discretization, Eq. 2.

2.2 Reconstruct-evolve-average

Another way to think about these methods is as a reconstruction, evolve, and average (R-E-A) process (see Figure 6).

We can write the conservative update as:

$$a_i^{n+1} = a_i^n + \frac{\Delta t}{\Delta x} (u a_{i-1/2}^{n+1/2} - u a_{i+1/2}^{n+1/2}) \quad (26)$$

$$= a_i^n + C(a_{i-1/2}^{n+1/2} - a_{i+1/2}^{n+1/2}) \quad (27)$$

If we take $u > 0$, then the Riemann problem will always choose the left state, so we can write this as:

$$a_i^{n+1} = a_i^n + C \left[\left(a_{i-1}^n + \frac{1}{2}(1 - C)\Delta a_{i-1} \right) - \left(a_i^n + \frac{1}{2}(1 - C)\Delta a_i \right) \right] \quad (28)$$

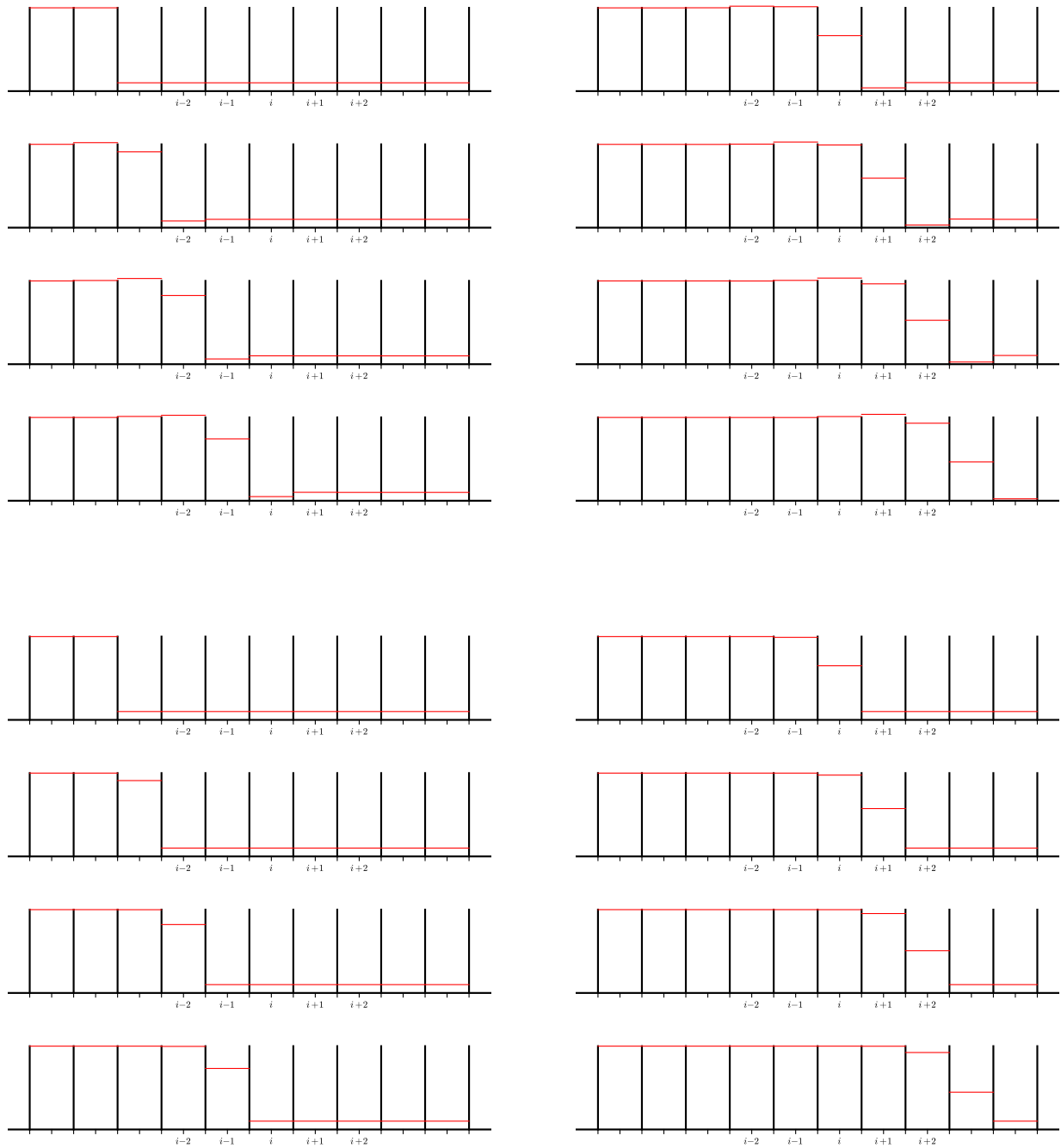


Figure 4: Initially discontinuous data evolved for several steps with no limiting (top sequence) and limiting (bottom sequence). Note that without limiting, there are overshoots and undershoots surrounding the discontinuity, and that the discontinuity remains sharper with limiting.

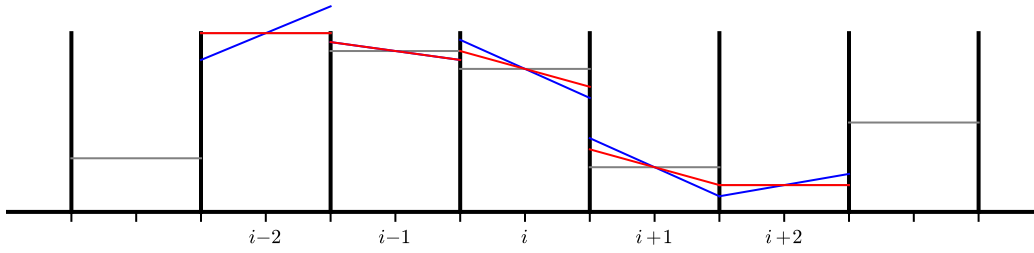


Figure 5: A finite-volume grid showing the cell averages (gray horizontal lines), unlimited center-difference slopes (blue) and MC limited slopes (red). Note that in zones i and $i + 1$, the slopes are limited slightly, so as not to overshoot or undershoot the neighboring cell value. Cell $i - 1$ is not limited at all, whereas cells $i - 2$, and $i + 2$ are fully limited—the slope is set to 0—these are extrema.

If we instead look at this via the R-E-A procedure, we write the reconstructed a in each zone in the form of a piecewise linear polynomial

$$a_i(x) = a_i + \frac{\Delta a}{\Delta x}(x - x_i) \quad (29)$$

Consider zone i . If we are advecting with a CFL number C , then that means that the fraction C of the zone immediately to the left of the $i - 1/2$ interface will advect into zone i over the timestep. And only the fraction $1 - C$ in zone i immediately to the right of the interface will stay in that zone. This is indicated by the shaded regions in Figure 6.

The average of the quantity a from zone $i - 1$ that will advect into zone i is

$$\mathcal{I}_< = \frac{1}{C\Delta x} \int_{x_{i-1/2}-C\Delta x}^{x_{i-1/2}} a_{i-1}(x) dx \quad (30)$$

$$= \frac{1}{C\Delta x} \int_{x_{i-1/2}-C\Delta x}^{x_{i-1/2}} \left[a_{i-1} + \frac{\Delta a_{i-1}}{\Delta x}(x - x_{i-1}) \right] dx \quad (31)$$

$$= a_{i-1} + \frac{1}{2}\Delta a_{i-1}(1 - C) \quad (32)$$

And the average of the quantity a in zone i that will remain in zone i is

$$\mathcal{I}_> = \frac{1}{(1 - C)\Delta x} \int_{x_{i-1/2}}^{x_{i-1/2}+(1-C)\Delta x} a_i(x) dx \quad (33)$$

$$= \frac{1}{(1 - C)\Delta x} \int_{x_{i-1/2}}^{x_{i-1/2}+(1-C)\Delta x} \left[a_i + \frac{\Delta a_i}{\Delta x}(x - x_i) \right] dx \quad (34)$$

$$= a_i - \frac{1}{2}\Delta a_i C \quad (35)$$

The final part of the R-E-A procedure is to average the over the advected profiles in the new cell. The weighted average of the average brought in from the left of the interface and that that remains in the cell is

$$a_i^{n+1} = C\mathcal{I}_< + (1 - C)\mathcal{I}_> \quad (36)$$

This is identical to Eq. 28. This demonstrates that the R-E-A procedure is equivalent to our reconstruction, prediction of the interface states, solving the Riemann problem, and doing the conservative flux update.

3 Errors and convergence rate

For the advection problem, the analytic solution is to simply propagate the initial profile to the right. This means that with periodic boundary condition, after advecting for one period, our numerical solution

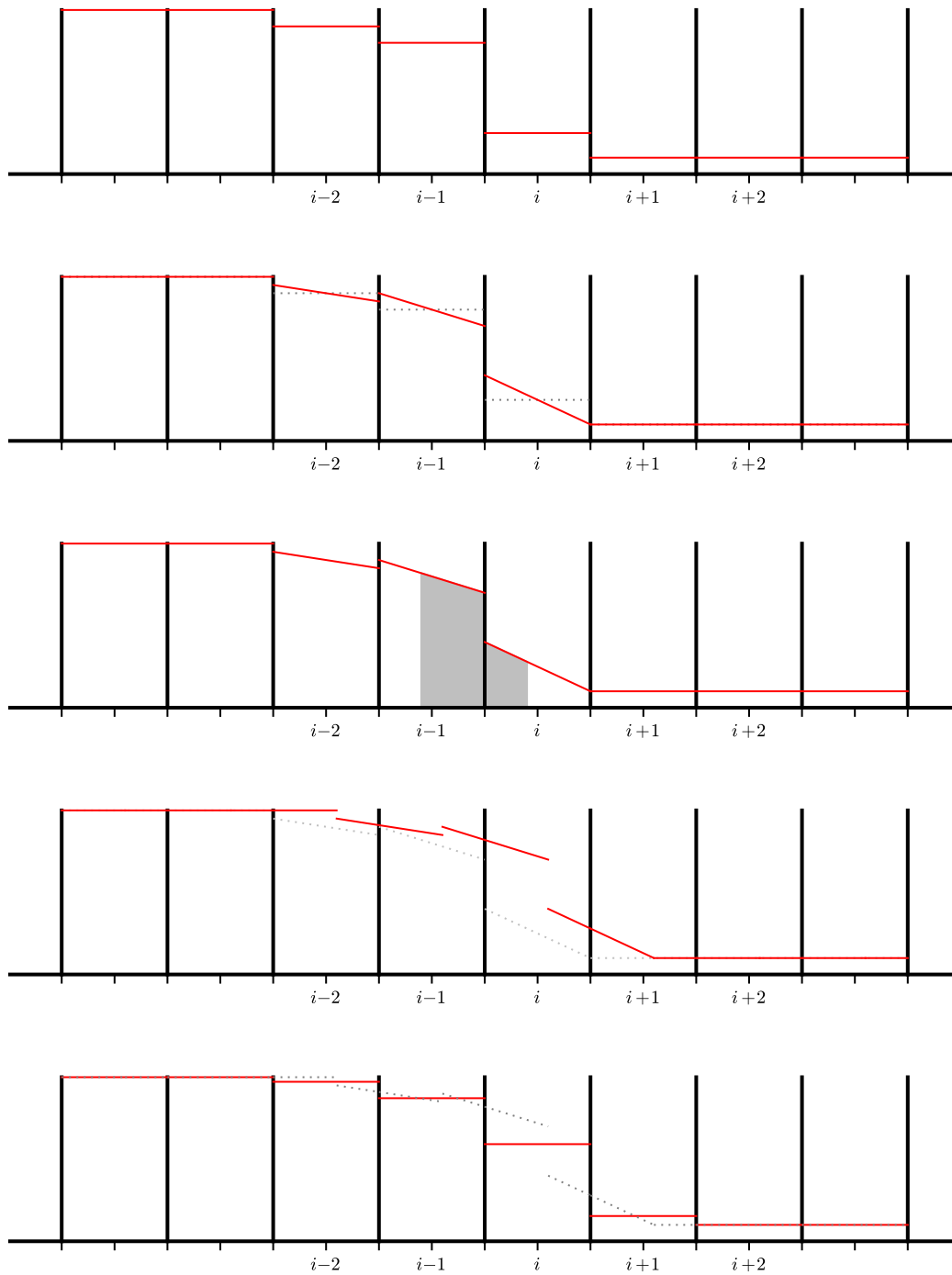


Figure 6: Reconstruct-Evolve-Average. The top panel shows the original cell-average data. The second panel shows the (limited) piecewise linear reconstruction of the data. Assuming a CFL number of 0.6 and advection to the right, the shaded regions in the third panel show the data that will wind up in cell i after advecting for a single step. The fourth panel shows the piecewise-linear data advected to the right by 0.6 of a cell-width (corresponding to a CFL of 0.6). The final panel shows the new averages of the data, constructed by averaging the advected piecewise linear data in each cell.

should be identical to the initial conditions. Any differences are our numerical error. We can quantify the error by taking the norm of error as: This is the L_2 -norm of the relative error. Sometimes we instead look at the norm of the absolute error:

$$\epsilon^{\text{abs}} = \|a^{\text{final}} - a^{\text{init}}\|_2 \equiv \left[\frac{1}{N} \sum_{i=1}^N (a_i^{\text{final}} - a_i^{\text{init}})^2 \right]^{1/2} \quad (37)$$

It is sometimes useful to compare to the norm of the original solution to get a measure of the relative error:

$$\epsilon^{\text{rel}} \equiv \frac{\|a^{\text{final}} - a^{\text{init}}\|_2}{\|a^{\text{init}}\|_2} \quad (38)$$

Note that it is important in these definitions to normalize by the number of zones, N , otherwise our error will be resolution-dependent.

Exercise 9: Run the first-order solver for several different Δx s, each a factor of 2 smaller than the previous. Compute ϵ for each resolution and observe that it converges in a first-order fashion (i.e. ϵ decreases by 2 when we decrease Δx by a factor of 2).

Do the same with the second-order solver and observe that it converges as second-order.

4 Multi-dimensional advection

The two-dimensional linear advection equation is:

$$a_t + ua_x + va_y = 0 \quad (39)$$

where u is the velocity in the x -direction and v is the velocity in the y -direction. We denote the average of $a(x, y, t)$ in a zone i, j as $a_{i,j}$. Here, i is the index in the x -direction and j is the index in the y -direction. A 2-d grid is shown in Figure 7. Just as in the one-dimensional case, we will extend the domain with a perimeter of ghost cells to set the boundary conditions.

We can discretize our equation by first integrating over the zones, recognizing that:

$$a_{i,j} = \frac{1}{\Delta x \Delta y} \int_{x_{i-1/2}}^{x_{i+1/2}} \int_{y_{j-1/2}}^{y_{j+1/2}} a(x, y, t) dx dy \quad (40)$$

Integrating Eq. 39 over x and y , we have:

$$\begin{aligned} \frac{1}{\Delta x \Delta y} \int_{x_{i-1/2}}^{x_{i+1/2}} \int_{y_{j-1/2}}^{y_{j+1/2}} a_t dx dy &= - \frac{1}{\Delta x \Delta y} \int_{x_{i-1/2}}^{x_{i+1/2}} \int_{y_{j-1/2}}^{y_{j+1/2}} (ua)_x dx dy \\ &\quad - \frac{1}{\Delta x \Delta y} \int_{x_{i-1/2}}^{x_{i+1/2}} \int_{y_{j-1/2}}^{y_{j+1/2}} (va)_y dx dy \end{aligned} \quad (41)$$

or

$$\frac{\partial a_{i,j}}{\partial t} = - \frac{1}{\Delta x} \{ (ua)_{i+1/2,j} - (ua)_{i-1/2,j} \} - \frac{1}{\Delta y} \{ (va)_{i,j+1/2} - (va)_{i,j-1/2} \} \quad (42)$$

Discretizing in time by evaluating the interface states at $n + 1/2$ (to achieve second-order accuracy), we have:

$$\frac{a_{i,j}^{n+1} - a_{i,j}^n}{\Delta t} = - \frac{(ua)_{i+1/2,j}^{n+1/2} - (ua)_{i-1/2,j}^{n+1/2}}{\Delta x} - \frac{(va)_{i,j+1/2}^{n+1/2} - (va)_{i,j-1/2}^{n+1/2}}{\Delta y} \quad (43)$$

There are two methods for computing the interface states: dimensionally split and unsplit. Dimensionally split methods are easier to code, since each dimension is operated on independent of the others, so you can simply call a one-dimensional method for each direction. Unsplit methods, however, are more accurate and less susceptible to grid effects.

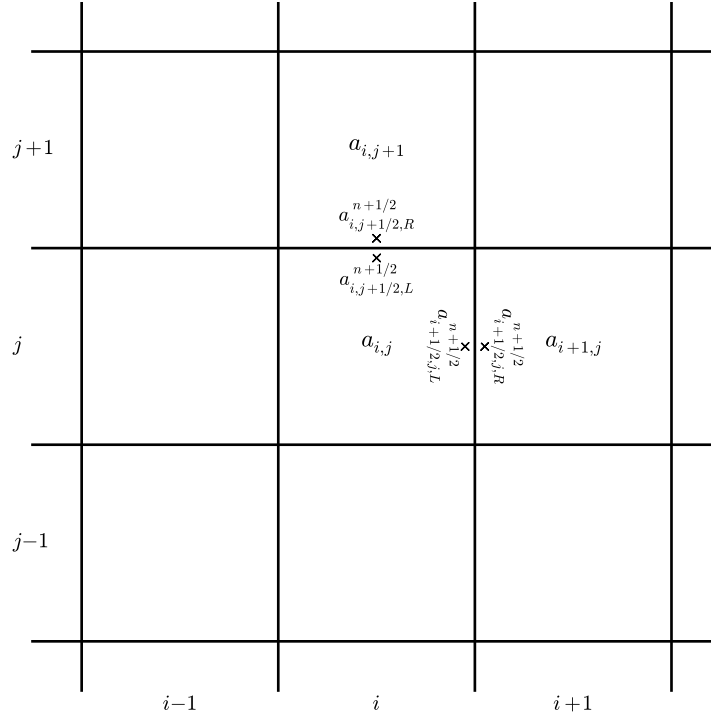


Figure 7: A simple 2-d grid with the zone-centered indexes. The \times s mark the interface states at the upper edge of the i, j zone in each coordinate direction.

4.1 Dimensionally split

In a split method, we update the state in each coordinate direction independently. This is simple and a straightforward way to use one-dimensional methods in multi-d. To be second-order accurate in time, we do *Strang splitting*, where we alternate the order of the dimensional updates each timestep. An update through Δt consists of x and y sweeps and appears as:

$$\frac{a_{i,j}^* - a_{i,j}^n}{\Delta t} = - \frac{ua_{i+1/2,j}^{n+1/2} - ua_{i-1/2,j}^{n+1/2}}{\Delta x} \quad (44)$$

$$\frac{a_{i,j}^{n+1} - a_{i,j}^*}{\Delta t} = - \frac{va_{i,j+1/2}^{*,n+1/2} - va_{i,j-1/2}^{*,n+1/2}}{\Delta y} \quad (45)$$

Here, Eq. 44 is the update in the x -direction. In constructing the interface states, $a_{i+1/2,j}^{n+1/2}$ and $a_{i-1/2,j}^{n+1/2}$, we do the exact same procedure as the one-dimensional case, constructing the left and right states at each interface and then solving the same Riemann problem to find the unique state on the interface. Each dimensional sweep is done without knowledge of the other dimensions. For example, in the x -update, we are solving:

$$a_t + ua_x = 0 \quad (46)$$

and in the y -update, we are solving:

$$a_t + va_y = 0 \quad (47)$$

The construction of the interface states largely mimics the one-dimensional case (Eq. 17 and 18). For example, the $a_{i+1/2,j,L}^{n+1/2}$ state is:

$$a_{i+1/2,j,L}^{n+1/2} = a_{i,j}^n + \frac{\Delta x}{2} \frac{\partial a}{\partial x} \Big|_{i,j} + \frac{\Delta t}{2} \frac{\partial a}{\partial t} \Big|_{i,j} + \mathcal{O}(\Delta x^2) + \mathcal{O}(\Delta t^2)$$

$$\begin{aligned}
&= a_{i,j}^n + \frac{\Delta x}{2} \frac{\partial a}{\partial x} \Big|_{i,j} + \frac{\Delta t}{2} \left(-u \frac{\partial a}{\partial x} \Big|_{i,j} \right) + \dots \\
&= a_{i,j}^n + \frac{\Delta x}{2} \left(1 - \frac{\Delta t}{\Delta x} u \right) \frac{\partial a}{\partial x} \Big|_{i,j} + \dots
\end{aligned} \tag{48}$$

Notice that when substituting for $\partial a / \partial t$, we use the one-dimensional split version of the advection equation (Eq. 46) instead of the full multi-dimensional equation. There are no y -direction terms that come into play in the split method when considering the x -direction.

The x -update (Eq. 44) updates the state only accounting for the x -fluxes—we denote this intermediate state with the ‘ \star ’ superscript. For the y -update, we construct our interface states in the analogous way as in the x -direction, but begin with the ‘ \star ’ state instead of the old-time state. In this fashion, the y -update ‘sees’ the result of the x -update and couples things together.

To achieve second-order accuracy in time, it is necessary to alternate the directions of the sweeps each timestep, i.e. x - y then y - x . Furthermore, this pair of sweeps should use the same timestep, Δt .

4.2 Unsplit multi-dimensional advection

The unsplit case differs from the dimensionally split case in two ways: (1) in predicting the interface states, we use knowledge of the transverse direction, and (2), only a single conservative update is done per timestep, with all directions updating simultaneously.

The construction of the $a_{i+1/2,j,L}^{n+1/2}$ interface state appears as

$$\begin{aligned}
a_{i+1/2,j,L}^{n+1/2} &= a_{i,j}^n + \frac{\Delta x}{2} \frac{\partial a}{\partial x} \Big|_{i,j} + \frac{\Delta t}{2} \frac{\partial a}{\partial t} \Big|_{i,j} + \mathcal{O}(\Delta x^2) + \mathcal{O}(\Delta t^2) \\
&= a_{i,j}^n + \frac{\Delta x}{2} \frac{\partial a}{\partial x} \Big|_{i,j} + \frac{\Delta t}{2} \left(-u \frac{\partial a}{\partial x} \Big|_{i,j} - v \frac{\partial a}{\partial y} \Big|_{i,j} \right) + \dots \\
&= a_{i,j}^n + \frac{\Delta x}{2} \left(1 - \frac{\Delta t}{\Delta x} u \right) \frac{\partial a}{\partial x} \Big|_{i,j} \underbrace{- \frac{\Delta t}{2} v \frac{\partial a}{\partial y} \Big|_{i,j}}_{\text{“transverse flux difference”}} + \dots
\end{aligned} \tag{49}$$

The main difference between the split and unsplit interface states is the explicitly appearance of the “transverse flux difference” in the unsplit interface state. We rewrite this as:

$$a_{i+1/2,j,L}^{n+1/2} = \hat{a}_{i+1/2,j,L}^{n+1/2} - \frac{\Delta t}{2} v \frac{\partial a}{\partial y} \Big|_{i,j} \tag{50}$$

Here, the $\hat{a}_{i+1/2,j,L}^{n+1/2}$ term is just the normal prediction without considering the transverse direction—this is constructed identically to the one-dimensional and split method. We compute these one-dimensional \hat{a} ’s at the left and right every interface in both coordinate directions. Note that these states are still one-dimensional, since we have not used any information from the transverse direction in their computation.

We then solve a Riemann problem at each of these interfaces:

$$a_{i+1/2,j}^T = \mathcal{R}(\hat{a}_{i+1/2,j,L}^{n+1/2}, \hat{a}_{i+1/2,j,R}^{n+1/2}) \tag{51}$$

$$a_{i,j+1/2}^T = \mathcal{R}(\hat{a}_{i,j+1/2,L}^{n+1/2}, \hat{a}_{i,j+1/2,R}^{n+1/2}) \tag{52}$$

$$\tag{53}$$

These states are given the T superscript since they are the states that are used in computing the transverse flux difference. Once we have the transverse state at every interface, we can correct the previously

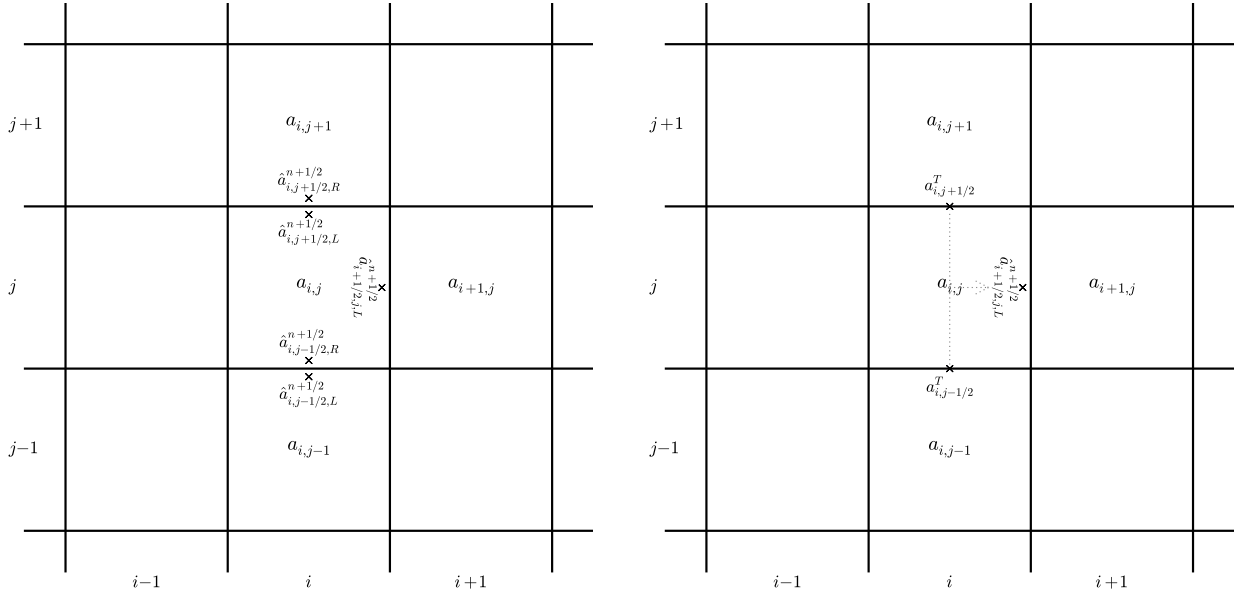


Figure 8: The construction of the $a_{i+1/2,j,L}^{n+1/2}$ state. Left: first we compute the \hat{a} 's—here we show all of the \hat{a} 's that will be used in computing the full left interface state at $(i + 1/2, j)$. Right: after the transverse Riemann solves, we have the two transverse states ($a_{i,j+1/2}^T$ and $a_{i,j-1/2}^T$) that will be differenced and used to correct $\hat{a}_{i+1/2,j,L}^{n+1/2}$ (illustrated by the dotted lines) to make $a_{i+1/2,j,L}^{n+1/2}$.

computed normal interface states (the \hat{a} 's) with the transverse flux difference:

$$a_{i+1/2,j,L}^{n+1/2} = \hat{a}_{i+1/2,j,L}^{n+1/2} - \frac{\Delta t}{2} v \frac{a_{i,j+1/2}^T - a_{i,j-1/2}^T}{\Delta y} \quad (54)$$

A similar procedure happens at the y -interfaces. Notice that the fluxes that are differenced for the left state are those that are transverse, but to the left of the interface. Similarly, for the right state, it would be those that are transverse, but to the right of the interface:

$$a_{i+1/2,j,R}^{n+1/2} = \hat{a}_{i+1/2,j,R}^{n+1/2} - \frac{\Delta t}{2} v \frac{a_{i+1,j+1/2}^T - a_{i+1,j-1/2}^T}{\Delta y} \quad (55)$$

Figure 8 illustrates the steps involved in the construction of the $a_{i+1/2,j,L}^{n+1/2}$ state.

Once all of the full states (normal prediction + transverse flux difference) are computed to the left and right of all the interfaces (x and y), we solve another Riemann problem to find the final state on each interface.

$$a_{i+1/2,j}^{n+1/2} = \mathcal{R}(a_{i+1/2,j,L}^{n+1/2}, a_{i+1/2,j,R}^{n+1/2}) \quad (56)$$

The final conservative update is then done via Eq. 43.

See [3] for more details on this unsplit method.

5 Going further

- *Stability analysis*: many texts provide the details of von Neumann stability analysis for the linear advection equation. There, you will see how a Fourier analysis can be used to derive the CFL condition. Note: this stability analysis is restricted to linear equations, but we nevertheless use the resulting limits for nonlinear equations (like the Euler equations).

- *Slope limiting*: there are a wide variety of slope limiters. All of them are designed to reduce oscillations in the presence of discontinuities or extrema, but some are higher-order and can be less restrictive when dealing with smooth flows. Most hydro texts (e.g. [5, 7]) provide an introduction to the design of such limiters.
- *Multi-dimensional limiting*: the procedure described above still does the limiting in each dimension independent of the other when doing the unsplit reconstruction. This can lead to overshoots/ undershoots. An example of a method that considers the limiting in multidimensions is [1, 6].

References

- [1] J. B. Bell, C. N. Dawson, and G. R. Shubin. An unsplit, higher order Godunov method for scalar conservation laws in multiple dimensions. 74:1–24, 1988.
- [2] P. Colella. A direct Eulerian MUSCL scheme for gas dynamics. *SIAM J Sci Stat Comput*, 6(1):104–117, 1985.
- [3] P. Colella. Multidimensional upwind methods for hyperbolic conservation laws. *Journal of Computational Physics*, 87:171–200, March 1990.
- [4] C. B. Laney. *Computational Gasdynamics*. Cambridge, 1998.
- [5] Randall J. LeVeque. *Finite-Volume Methods for Hyperbolic Problems*. Cambridge University Press, 2002.
- [6] S. May, A. J. Nonaka, A. S. Almgren, and J. B. Bell. An unsplit, higher order Godunov method using quadratic reconstruction for advection in multiple dimensions. *Communications in Applied Mathematics and Computational Science*, 6(1), 2011.
- [7] E. F. Toro. *Riemann Solvers and Numerical Methods for Fluid Dynamics*. Springer, 1997.